Old Dominion University
ODU Digital Commons

OES Faculty Publications | Ocean & Earth Sciences

2-2017

Multiple Metabolisms Constrain the Anaerobic Nitrite Budget in the Eastern Tropical South Pacific

Andrew R. Babbin

Brian D. Peters

Calvin W. Mordy

Brittany Widner
Old Dominion University, bwidn001@odu.edu

Karen L. Casciotti

See next page for additional authors

Follow this and additional works at: https://digitalcommons.odu.edu/oeas_fac_pubs

Part of the Atmospheric Sciences Commons, Biogeochemistry Commons, Environmental Sciences Commons, and the Oceanography Commons

Original Publication Citation

Babbin, A. R., Peters, B. D., Mordy, C. W., Widner, B., Casciotti, K. L., & Ward, B. B. (2017). Multiple metabolisms constrain the anaerobic nitrite budget in the Eastern Tropical South Pacific. *Global Biogeochemical Cycles, 31*(2), 258-271. doi:10.1002/2016GB005407

This Article is brought to you for free and open access by the Ocean & Earth Sciences at ODU Digital Commons. It has been accepted for inclusion in OES Faculty Publications by an authorized administrator of ODU Digital Commons. For more information, please contact digitalcommons@odu.edu.

Authors
Andrew R. Babbin, Brian D. Peters, Calvin W. Mordy, Brittany Widner, Karen L. Casciotti, and Bess B. Ward

This article is available at ODU Digital Commons: https://digitalcommons.odu.edu/oeas_fac_pubs/226

AGU PUBLICATIONS

Global Biogeochemical Cycles

RESEARCH ARTICLE

10.1002/2016GB005407

Key Points:
- Directly measured in situ rates produce the broad nitrogen profiles in ODZs assuming contributions from both anammox and denitrification
- Nitrite and nitrate are rapidly cycled in ODZs, and iodate stimulates nitrite oxidation in the upper ODZ
- Cyanate can act as a reduced nitrogen source for anammox, while urea is not directly used

Supporting Information:
- Supporting Information S1
- Table S1

Correspondence to:
A. R. Babbin,
babbin@mit.edu

Citation:
Babbin, A. R., B. D. Peters, C. W. Mordy, B. Widner, K. L. Casciotti, and B. B. Ward (2017), Multiple metabolisms constrain the anaerobic nitrite budget in the Eastern Tropical South Pacific, *Global Biogeochem. Cycles*, *31*, 258–271, doi:10.1002/2016GB005407.

Received 3 MAR 2016
Accepted 29 DEC 2016
Accepted article online 26 JAN 2017
Published online 4 FEB 2017

©2017. American Geophysical Union. All Rights Reserved.

Multiple metabolisms constrain the anaerobic nitrite budget in the Eastern Tropical South Pacific

Andrew R. Babbin[1,2], Brian D. Peters[3], Calvin W. Mordy[4,5], Brittany Widner[6], Karen L. Casciotti[3], and Bess B. Ward[2]

[1]Department of Earth, Atmospheric, and Planetary Sciences, Massachusetts Institute of Technology, Cambridge, Massachusetts, USA, [2]Department of Geosciences, Princeton University, Princeton, New Jersey, USA, [3]Department of Earth System Science, Stanford University, Stanford, California, USA, [4]Pacific Marine Environmental Laboratory, National Oceanic and Atmospheric Administration, Seattle, Washington, USA, [5]Joint Institute for the Study of the Atmosphere and Ocean, University of Washington, Seattle, Washington, USA, [6]Department of Ocean, Earth and Atmospheric Sciences, Old Dominion University, Norfolk, Virginia, USA

Abstract The Eastern Tropical South Pacific is one of the three major oxygen deficient zones (ODZs) in the global ocean and is responsible for approximately one third of marine water column nitrogen loss. It is the best studied of the ODZs and, like the others, features a broad nitrite maximum across the low oxygen layer. How the microbial processes that produce and consume nitrite in anoxic waters interact to sustain this feature is unknown. Here we used ^{15}N-tracer experiments to disentangle five of the biologically mediated processes that control the nitrite pool, including a high-resolution profile of nitrogen loss rates. Nitrate reduction to nitrite likely depended on organic matter fluxes, but the organic matter did not drive detectable rates of denitrification to N_2. However, multiple lines of evidence show that denitrification is important in shaping the biogeochemistry of this ODZ. Significant rates of anaerobic nitrite oxidation at the ODZ boundaries were also measured. Iodate was a potential oxidant that could support part of this nitrite consumption pathway. We additionally observed N_2 production from labeled cyanate and postulate that anammox bacteria have the ability to harness cyanate as another form of reduced nitrogen rather than relying solely on ammonification of complex organic matter. The balance of the five anaerobic rates measured—anammox, denitrification, nitrate reduction, nitrite oxidation, and dissimilatory nitrite reduction to ammonium—is sufficient to reproduce broadly the observed nitrite and nitrate profiles in a simple one-dimensional model but requires an additional source of reduced nitrogen to the deeper ODZ to avoid ammonium overconsumption.

1. Introduction

Nitrite is the central compound to many pathways in the marine nitrogen cycle—it is produced and consumed during nitrification; it is an intermediate during nitrate assimilation by phytoplankton; it is the product of dissimilatory nitrate reduction; and it is the substrate for anammox, denitrification, and dissimilatory nitrite reduction to ammonium (DNRA). While ephemeral nitrite accumulation has been observed [*Mordy et al.*, 2010], nitrite occurs mostly in trace concentrations in the ocean, except at two depth horizons. (i) A primary nitrite maximum (PNM) on the order of a hundred nanomolar occurs across the stratified ocean at the base of the euphotic zone [*Lomas and Lipschultz*, 2006] and is thought to indicate an uncoupling of reduction steps during the assimilation of nitrate or an imbalance between the two steps of nitrification [*Olson*, 1981a, 1981b; *Buchwald and Casciotti*, 2013]. (ii) A much larger secondary nitrite maximum (SNM), which can reach levels as high as 10 μmol L^{-1}, exists only within the anoxic regions of the world's oxygen deficient zones (ODZs) [*Codispoti et al.*, 2001]. The origin of the SNM is not well understood, although it is observed in every ODZ. The SNM arises from an imbalance among the biological processes producing and consuming nitrite. Whether the nitrite in the SNM is rapidly generated or a historical remnant is unknown due to poorly constrained water residence time estimates, which range from a few months to a decade [*Codispoti et al.*, 2001; *DeVries et al.*, 2012], here we attempt to characterize the origin and maintenance of SNMs.

The major ODZs of the Eastern Tropical Pacific and the Arabian Sea comprise less than 0.1% of the ocean's volume [*Codispoti et al.*, 2001] but are responsible for approximately one third of marine fixed nitrogen loss [*Brandes and Devol*, 2002; *Gruber*, 2004; *Codispoti*, 2007], making them crucially important to global biogeochemistry and Earth's climate [*Ward*, 2013]. The Eastern Tropical South Pacific (ETSP) region extending off

the coasts of northern Chile and Peru is one such ODZ. This area is characterized by intense coastal upwelling that drives one of the largest nearshore fisheries in the world [*Cheung et al.*, 2010]. Beneath the highly productive surface layer, oxygen very sharply decreases to concentrations below 10 nmol L^{-1}, undetectable by conventional methods [*Revsbech et al.*, 2009]. Across this anoxic interval, which spans generally between 75 m and 400 m in depth, a strong SNM is consistently observed [*Friederich and Codispoti*, 1987; *Thamdrup et al.*, 2006; *Lam et al.*, 2009; *Casciotti et al.*, 2013]. The processes invoked to explain the SNM include an imbalance in production by dissimilatory nitrate reduction (the first step in denitrification) and consumption by anammox, DNRA, and the subsequent reduction steps in denitrification [*Lam et al.*, 2009; *Ward et al.*, 2009; *Lam and Kuypers*, 2011].

Recently, another potential nitrite consumption term, anaerobic nitrite oxidation, has been suggested to be significant in the ODZs on the basis of sparse rate measurements [*Lipschultz et al.*, 1990; *Füssel et al.*, 2011; *Beman et al.*, 2013; *Peng et al.*, 2015, 2016], modeled rates [*Lam et al.*, 2011], and natural abundance isotopic measurements [*Casciotti et al.*, 2013; *Buchwald et al.*, 2015]. Furthermore, anaerobic nitrite oxidation has been observed in culture experiments with *Nitrobacter* [*Lees and Simpson*, 1957; *Bock et al.*, 1988] and implicated as an electron donor for anoxygenic photosynthesis in a sewage sludge enrichment most likely associated with the *Thiocapsa* genus [*Griffin et al.*, 2007]. While photosynthesis may provide oxidative power at certain sites where the oxycline is shallower than the 1% light level, the possible mechanisms supporting anaerobic nitrite oxidation in the dark SNM environment are unknown. Potential alternative oxidants include iodate, a relatively abundant and active compound in the global ocean with concentrations approximately 0.5 μmol L^{-1} on average [*Nozaki*, 1997; *Lam and Kuypers*, 2011]. In the Arabian Sea ODZ, a region analogous to the ETSP, there is evidence that reduction of iodate to iodide occurs within the anoxic depths, with up to 0.5 μmol L^{-1} iodide accumulation [*Farrenkopf and Luther*, 2002]. While this signal may be caused by the reductive versatility of denitrifying organisms whereby bacteria reduce nitrate and iodate as observed in marine *Shewanella* [*Farrenkopf et al.*, 1997] and *Pseudomonas* [*Amachi et al.*, 2007] cultures, the oxidative power of iodate might also fuel nitrite oxidation.

In addition to alternative nitrite oxidants, another component of uncertain importance to the ODZ nitrogen cycle is the supply of reduced nitrogen (i.e., ammonium and urea) to depth by vertically migrating zooplankton. Numerous studies have documented significant zooplankton abundances in these coastal upwelling zones [*Wishner et al.*, 1998, 2008, 2013]. Further, these populations migrate daily, feeding at the surface at night and spending the day at depth, often within the anoxic ODZ core [*Steinberg et al.*, 2002; *Bianchi et al.*, 2013]. Recent modeling work has suggested that zooplankton excretion can influence nitrogen biogeochemistry by augmenting anammox rates relative to denitrification [*Bianchi et al.*, 2014].

The present study in the ETSP off the northern Chilean coast (Figure S1 in the supporting information) aims (1) to provide a nitrite budget for the SNM and (2) to assess the net rate of nitrite accumulation by directly measuring rates of the possible biological source (nitrate reduction) and sinks (anammox, denitrification, DNRA, and nitrite oxidation) of nitrite in the anoxic layer. Fixed nitrogen loss at this site was investigated in detail by conducting high-resolution sampling (interval of 4–8 m in depth, 75 depths in total ranging from the surface to the bottom of the ODZ at 400 m) by using an in situ pump profiler (pump cast) of the anoxic water column for N_2 production incubations. Additional experiments amending site water with iodate, urea, and cyanate were conducted to determine the potential for these compounds to support novel nitrite consumption metabolisms within the ODZ.

2. Methods

2.1. Site Description and Sampling

Our study took place off the northern Chilean and Peruvian coasts (Figure S1) in July 2013 as part of an extensive survey of the ETSP oxygen deficient zone aboard the RVIB *Nathaniel B. Palmer*. The site selected for an intensive study with high depth resolution was located just off the shelf at 20.5°S 70.7°W and had a bottom depth of 1600 m. Two sampling methods were employed: water was collected from either a conductivity-temperature-depth rosette with 12 L Niskin bottles (for nitrate reduction and nitrite oxidation experiments) or from an in situ pumped profiler system (PPS) which was able to pump water from depths as deep as 400 m directly onboard with minimal oxygen contamination [*Canfield et al.*, 2010]. The PPS was operated at a flow rate of 2 L min^{-1} and descended at a rate of 4 m min^{-1}. The PPS was sampled on the downcast

for high-resolution nutrients as well as for anammox and denitrification rate incubations. Oxygen profiles were measured with a Seabird SBE45 electrode, with a nominal detection limit of 2 μmol L^{-1}. However, O_2 concentration measurements were also made with a Switchable Trace Oxygen sensor such that the ODZ was defined as the region with $O_2 < 10$ nmol L^{-1} [*Revsbech et al.*, 2009; *Tiano et al.*, 2014].

2.2. Nutrient Measurements

Nutrient samples were collected from the PPS for discrete NH_4^+, NO_2^-, NO_3^-, and PO_4^{3-} concentrations at a resolution of ~8 m. Nutrients were measured within hours of collection by using an autoanalyzer with standard photometric techniques [*Strickland and Parsons*, 1972; *Grasshoff*, 1983]. Separately, a line was plumbed directly from the continuous PPS flow to the autoanalyzer for near-continuous monitoring of NO_2^-. N* or the measured deficiency in fixed nitrogen relative to phosphate from a standard N:P ratio of 16:1 [*Gruber and Sarmiento*, 1997; *Deutsch et al.*, 2001] was calculated by the relationship $N^* = \left(\left[NO_3^-\right] + \left[NO_2^-\right] + \left[NH_4^+\right]\right) - 16\left[PO_4^{3-}\right]$. The commonly used offset of 2.9 μmol kg^{-1} to make the global average $N^* = 0$ [*Deutsch et al.*, 2001] was not included because relative changes with depth are important for our study.

2.3. Instantaneous Rate ^{15}N Tracer Experiments

Incubations for anammox and denitrification rates were conducted by plumbing the PPS seawater flow directly into a continuously flushed N_2 glove bag. At each sampling time point (every 1 or 2 min, corresponding to 4 or 8 m in depth interval, respectively), two 12 mL Exetainer vials (Labco, UK) were filled without turbulence to the brim and capped without allowing a bubble by piercing the septa with a 23 gauge needle. Upon finishing the collection (~2 h), helium was used to flush the vials for 5 min and 4 mL headspace was introduced into the vials. The vials for anammox and denitrification were amended by using a gastight syringe with a helium flushed tracer solution (final amendment concentrations were 3 μmol L^{-1} $^{15}NO_2^-$ (Cambridge Isotope Laboratories, MA, USA) and 3 μmol L^{-1} $^{14}NH_4^+$). Denitrification-only experiments were amended with $(^{15}N)_2O$ (Cambridge Isotope Laboratories, MA, USA) by using a gastight syringe to a final concentration of 50 nmol L^{-1}. The vials were incubated in the dark at 10°C for 24 h, and biological activity was stopped with 50 μL 50% (w/v) $ZnCl_2$. The limit of detection for denitrification was 2 nmol N_2 L^{-1} d^{-1} for the $(^{15}N)_2O$ experiments and between 1 and 14 nmol N_2 L^{-1} d^{-1} for the $^{15}NO_2^-$ experiments, depending on the ambient nitrite concentration. Limits of detection for total nitrogen loss were 0.1 to 0.4 nmol N_2 L^{-1} d^{-1}, depending on the nitrite concentration.

As only one vial was collected for each tracer, the rates were based on single endpoint determinations at 24 h, with an assumption that, at the initial time point, the N_2 present in the vials was unenriched in either $^{29}N_2$ or $^{30}N_2$. For these incubations, the N_2 samples were measured on a Europa 20/20 gas chromatography/isotope ratio mass spectrometer (GC/IRMS) as previously described [*Babbin et al.*, 2014]. Headspace from the $(^{15}N)_2O$-treated samples was first trapped in an in-line liquid N_2 trap prior to injection in the GC to remove unreduced N_2O. Rates were calculated by assuming a linear production of labeled nitrogen gas over 24 h (as previous work has shown to be a fair assumption in this region) [*Dalsgaard et al.*, 2012]. The N_2O substrate pool was assumed to be 100% labeled because the in situ N_2O was removed via helium purging before addition of the tracer labeled gas.

Separately, experiments for nitrite oxidation and nitrate reduction were performed as previously [*Babbin et al.*, 2014], amending site water collected in Niskin bottles from 5 depths with 3 μmol L^{-1} of either $^{15}NO_2^-$ or $^{15}NO_3^-$ for the nitrite oxidation or nitrate reduction incubations, respectively. A separate nitrite oxidation experiment with an iodate amendment was also performed, with KIO_3 added to a final concentration of 1 μmol L^{-1} in addition to the nitrite tracer. Incubations were performed in 12 mL Exetainer vials that were flushed with helium for 5 min to further minimize potential oxygen contamination arising from sampling. The vials were incubated in the dark at 10°C, and triplicate vials were sacrificed every 12 h over a 48 h total incubation period by the addition of 50 μL 50% (w/v) $ZnCl_2$ solution. Because we were interested in detecting an anaerobic transformation that is assumed to be obligately aerobic, and in light of the high affinity of NO_2^- oxidation for O_2 [*Bristow et al.*, 2016], extra precautions were taken to eliminate O_2. Seawater was sampled directly into ground glass O_2 bottles and opened only inside an N_2-filled glove bag. Further, the Exetainer septa was degassed and stored in an anoxic headspace for weeks prior to use.

Upon return to shore, nitrate reduction to nitrite time point samples were measured by converting the nitrite pool to N_2O with sodium azide [*McIlvin and Altabet*, 2005; *Newell et al.*, 2011] and measuring directly on a Finnigan Delta-V IRMS. Nitrite oxidation to nitrate experiments had excess labeled nitrite removed by using the sulfamic acid method [*Lipschultz et al.*, 1990; *Granger and Sigman*, 2009]. Aliquots (1 mL) of samples were treated with 10 μL 5% sulfamic acid for 1 h before neutralization with NaOH. During this reaction, the samples equilibrated with air such that any $^{15}N_2O$ produced by denitrifiers shipboard [*Babbin et al.*, 2015] was removed from the sample. The treated samples were then injected into denitrifier *Pseudomonas chlororaphis* [*Sigman et al.*, 2001] cultures, which converted the nitrate in solution to N_2O. N_2O was then measured on the same mass spectrometer as the nitrate reduction experiments.

Rates of production of either $^{15}NO_2^-$ from the nitrate reduction or $^{15}NO_3^-$ from the nitrite oxidation experiments were calculated by fitting the observed enrichments over time with a linear function and dividing by the fraction of labeled substrate (50 ± 25% for nitrite and 14 ± 3% for nitrate). These tracer concentrations may be potentially stimulating for the reaction rates measured, but given the nonlinear kinetics of enzymatic pathways, this effect is difficult to parse. Nevertheless, the microbes must be present and active within the incubations to detect any of the products measured. As opposed to single endpoint measurements, the time course incubations for nitrite oxidation and nitrate reduction allowed us to avoid experimental artifacts that assume an initial natural abundance isotopic composition. In so doing, we observed that the ^{15}N-labeled NO_2^- stock is likely contaminated with $^{15}NO_3^-$, with initial T_0 vials enriched up to 1000‰. Additionally, the sulfamic acid method is not 100% efficient in removing NO_2^-, so that will contribute to this initial offset [*Granger and Sigman*, 2009]. The change in enrichment of the product over time determines the rate, meaning this initial offset does not affect the rate calculation, assuming each replicate began with the same nitrite and nitrate concentrations and isotopic compositions. Moreover, any stochasticity in sulfamic acid efficiency will be accounted for in the replicability among triplicates and the standard error of the slope fit through the 15 independent Exetainer measurements.

Cyanate ($OC^{15}N^-$) and urea ($H_2{}^{15}NCO^{15}NH_2$) addition experiments utilized custom synthesized (Cambridge Isotope Laboratories, MA, USA) ^{15}N-labeled compounds. Amendments consisted of 3 μmol L^{-1} of cyanate or 1.5 μmol L^{-1} of urea (3 μmol L^{-1} of ^{15}N). These concentrations are much higher than those that naturally occur in the ocean but were chosen in order to standardize the amount of reduced nitrogen in the incubations. While the rates of utilization of these substrates may be potentially stimulated, detecting the oxidation of these substrates would show that the reaction is indeed possible in the marine environment. Incubations were performed and N_2 production rates measured as in other experiments.

2.4. One-Dimensional Advection-Diffusion-Reaction Model

A prognostic one-dimensional model of the oxygen deficient zone between the upper oxycline (75 m) and the lower oxycline (400 m) at 1 m vertical resolution was used to determine how the measured in situ rates affect nitrite and nitrate concentrations. The four measured rates of nitrite transformations were transformed to be functions of depth (see section 3 for details). Anammox and denitrification rates from the pump cast were interpolated to a 1 m resolution by using a simple linear interpolant between bounding measurements. A partitioning between the two N_2 production pathways was assumed by using a linear interpolation between measurements, with the fraction of anammox at depths shallower than 80 m being set to the shallowest measurement (80 m) and at depths deeper than 375 m to the deepest measurement (375 m). Nitrate reduction rates were fit to a power law scaling with depth, similar to organic matter consumption [*Martin et al.*, 1987; *Newell et al.*, 2011; *Babbin et al.*, 2014]. Nitrite oxidation rates were set by using a step function between measurements, given the lack of additional constraints to determine a more robust relationship with depth.

Advection and diffusion constants were determined from the observed temperature and salinity distributions [*Fennel and Boss*, 2003] such that $v = -2 \times 10^{-7}$ m s^{-1} (upwelling) and $D = 4 \times 10^{-5}$ m^2 s^{-1}. We assumed diffusivity to be constant with depth as per previous ODZ studies [*Yamagishi et al.*, 2007; *Babbin et al.*, 2015]. The full equations solved were

$$\frac{\partial NO_2^-}{\partial t} = D\frac{\partial^2 NO_2^-}{\partial^2 z} + v\frac{\partial NO_2^-}{\partial z} + \Sigma\left(R_z^{nar} - R_z^{amx} - R_z^{dnt} - R_z^{nxr}\right)$$

$$\frac{\partial NO_3^-}{\partial t} = D\frac{\partial^2 NO_3^-}{\partial^2 z} + v\frac{\partial NO_3^-}{\partial z} + \Sigma\left(R_z^{nxr} - R_z^{nar}\right)$$

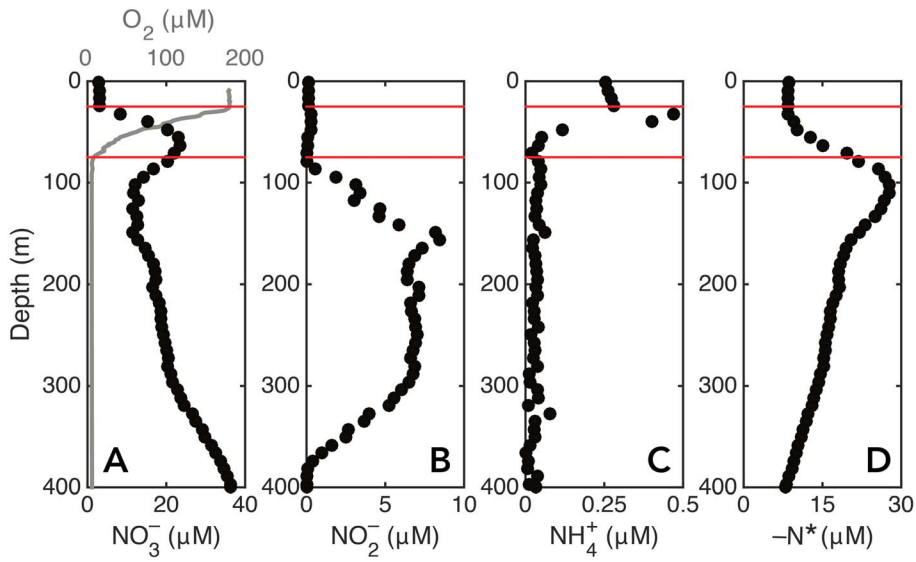

Figure 1. Nutrients measured from the pump cast. (a) Nitrate (circles) and dissolved oxygen (grey line), (b) nitrite, (c) ammonium, and (d) negative N* indicating DIN consumption relative to phosphate. The horizontal red lines delineate the upper and lower boundaries of the oxycline.

where R_z^i is the rate of process *i* at depth *z*. The abbreviations for each process are nitrate reduction (nar), anammox (amx), denitrification (dnt), and nitrite oxidation (nxr). The model was stepped forward in time (time step of 10^4 s) until the maximum modeled nitrite concentration equaled the measured, which occurred at 296 days. This model excluded horizontal advection, so the water mass modeled can be interpreted from a Lagrangian reference frame. Boundary conditions at the top and bottom of the ODZ were set to match measurements 0 μmol L^{-1} NO_2^- and NH_4^+ at both boundaries and 23 and 36.4 μmol L^{-1} NO_3^- at the top and bottom boundaries, respectively. Initial conditions for the model were zero nitrite and ammonium concentrations throughout the water column and 22 μmol L^{-1} nitrate deficit throughout the ODZ to match the observation at the base of the oxycline.

3. Results and Discussion

3.1. Water Column Physical and Biogeochemical Structure

The chemical structure of the water column (Figure 1) was consistent with previous reports for the ETSP ODZ [*Thamdrup et al.*, 2006; *Hamersley et al.*, 2007; *Lam et al.*, 2009; *Ward et al.*, 2009; *Chang et al.*, 2010]. A well-mixed surface layer (upper ~25 m) was evident from the nearly uniform water density and O_2 concentrations. Then, through a steep pycnocline (Figure S3), O_2 concentrations decreased through the oxycline to undetectable (anoxic) levels by 75 m. Oxygen remained undetectable until ~400 m, where its concentration increased again, although much more gradually than in the upper oxycline. Within this column of anoxic water was the characteristic decrease in nitrate concentrations (Figure 1a) and secondary nitrite maximum (Figure 1b), peaking at 8.5 μmol L^{-1} at 150 m. Ammonium concentrations were consistently below 80 nmol L^{-1} for all of the anoxic depths sampled (Figure 1c). The dissolved inorganic nitrogen (DIN) deficit peaked at 100 m (Figure 1d), shallower than the local nitrate minimum and nitrite maximum.

3.2. Anammox and Denitrification Rate Measurements

N_2 production from nitrite was detected throughout the depth interval where oxygen was below detection limits (Figure 2a). All of this nitrogen loss appears to be due to anammox because the measurement of dual-labeled N_2 gas that indicates denitrification and DNRA were below the detection limit of 4 nmol N L^{-1} d^{-1} at this station (Figure 2b). Separately measured N_2O production rates from nitrite and nitrate reduction confirm that denitrification rates range between 3.5 nmol L^{-1} d^{-1} at the top of the ODZ and 1 nmol L^{-1} d^{-1} at the bottom [*Ji et al.*, 2015]. While anammox has been reported as the sole N_2 production process in the ETSP in numerous other studies [*Thamdrup et al.*, 2006; *Lam et al.*, 2009; *Ward et al.*, 2009], denitrification has

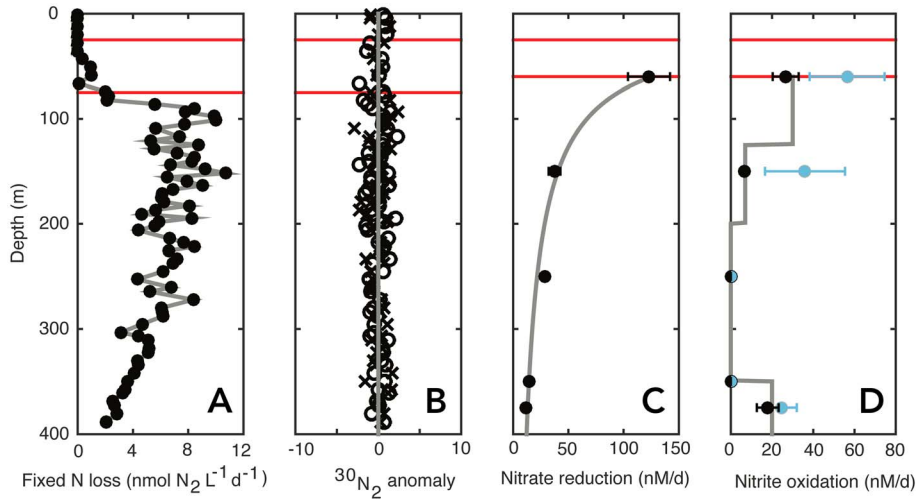

Figure 2. Measurements of nitrogen transformation. (a) Nitrogen loss rates from $^{15}NO_2^-$ tracer incubations. (b) $^{30}N_2$ production relative to the mean signal where the anomaly, $\hat{x} = \frac{x_i - \bar{x}}{s_x}$ for $^{15}NO_2^-$ (o) and $^{46}N_2O$ (x) treatments, respectively. (c) Nitrate reduction rates from bottle sampling. (d) Nitrite oxidation rates from bottle sampling. Nitrite oxidation experiments without additional IO_3^- are in black, while those with amendments are in blue. The error bars denote standard errors in slope through 15 points (5 time points in triplicate). For all panels, the grey curves show parameterizations with depth used in our 1-D biogeochemical model. The horizontal red lines delineate the upper and lower boundaries of the oxycline. Samples for nitrate reduction and nitrite oxidation (Figures 2 and 2d) are from a different day where internal physical dynamics shifted the water column structure slightly, which is why the oxycline is slightly different from that of the pump cast.

also been observed in this region, albeit sporadically but at high rates [*Dalsgaard et al.*, 2012; *Kalvelage et al.*, 2013], and a stoichiometrically balanced partitioning between the two modes of fixed nitrogen loss is more likely [*Babbin et al.*, 2014].

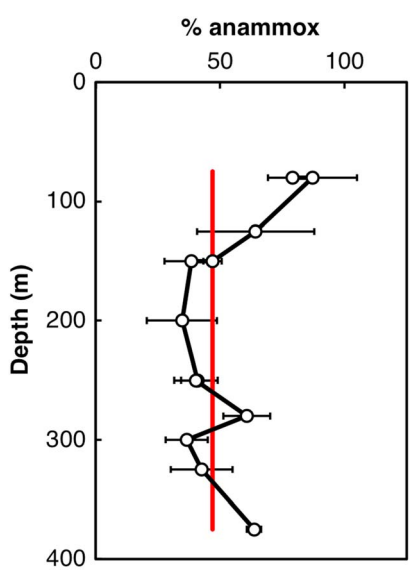

Figure 3. The contribution of anammox to N_2 loss from additional measurements at this station. Measurements of anammox percentage from the coastal ETSP site are shown. The error bars indicate propagated error from 15 N_2 production measurements parsed into anammox and denitrification [*Babbin et al.*, 2014]. The profile is a compilation of 12 separate depths (9 unique) sampled over three different days. The vertical red line denotes the 47% average anammox contribution observed below 100 m depth. Details are provided in the supporting information.

The method for partitioning nitrogen loss presented here and previously [*Thamdrup et al.*, 2006; *Lam et al.*, 2009; *Dalsgaard et al.*, 2012] suffers from a high detection limit for conclusively determining denitrification rates by the appearance of dual-labeled $^{30}N_2$ in our incubations. The overall rates are slow, and the high in situ nitrite concentration background limits the fraction of N_2 generation that proceeds into the $^{30}N_2$ pool, factors which collude to limit detectability. However, for a variety of reasons, denitrification is likely to represent a significant portion of the observed N_2 production in our experiments. From the multiple independent lines of evidence presented below, we conclude that an anammox-only regime is unrealistic and proceed with our analysis without differentiating between the two nitrogen loss pathways.

(i) Other measurements conducted at this site with a higher sensitivity for denitrification (supporting information) but at a lower vertical resolution indicate that an average fraction of anammox should be 47 ± 4% within the core of the ODZ (Figure 3). Higher relative amounts of anammox were observed in the

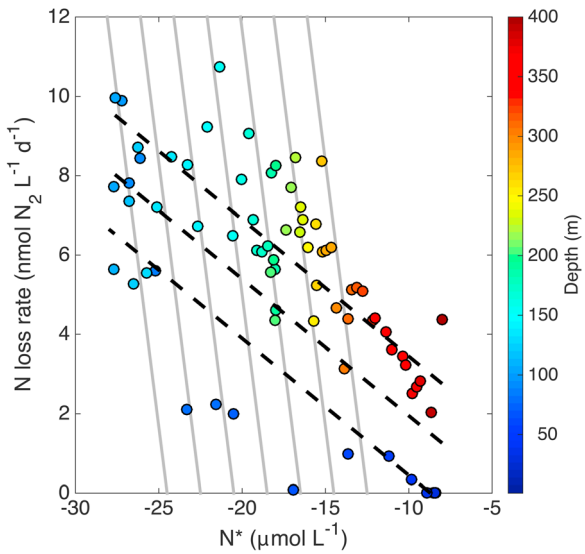

Figure 4. Relationship between nitrogen loss rates and fixed nitrogen deficit (N*). Depths are indicated by color, and the dashed black lines indicate the best fit regression slope through all data, $R_{\text{N loss}} = \frac{N^*}{8\text{ years}}$. The solid grey contours indicate the slope expected if the measured nitrogen loss rates were to generate the observed nitrogen deficits in 296 days, from different starting points on the N* axis.

upper and lower ODZs, possibly due to low but significant O_2 concentrations (10s to 100 s nmol L^{-1}) [*Dalsgaard et al.*, 2014]. The representative profile shown was from the same station as the pump cast, but data from across the ETSP cruise indicate the same trend with similar anammox fractions.

(ii) A role for denitrification is further corroborated by simultaneously measured nutrients and natural abundance isotope measurements from the pump cast, which predict contributions from both anammox and denitrification for this ODZ [*Peters et al.*, 2016].

(iii) A third piece of evidence that processes (i.e., denitrification) in addition to what anammox contributes to the production of N_2 is observed when modeling our measured N_2 production rates, assuming that all of the N_2 produced is from only anammox: in this model setup, ammonium is greatly and unrealistically over consumed (Figure S2), as further described in section 4.

In the high-resolution pump cast, nitrogen loss rates increased substantially once O_2 disappeared at ~75 m, were maximal near the top of the ODZ (~100 m), and decreased with depth. Interestingly, the potential for low rates of anammox just below the PNM in the oxycline (~50 m) is apparent from these measurements (Figure 2a), as previously observed for this region [*De Brabandere et al.*, 2014]. Because O_2 concentrations were reduced below ambient levels by the methodological protocols in the surface-most incubations, however, whether the anammox and denitrifying bacteria were active at higher ambient O_2 conditions cannot be definitively assessed. Still, active rates of nitrogen loss are potentially responsible for some of the nitrite and ammonium consumptions seen below the concentration peaks of nitrite and ammonium in the surface ocean (Figure 1).

Nitrogen loss rates correlated significantly with the integrated nitrogen deficit (N*), which is an independent geochemical measurement of fixed nitrogen loss ($p \ll 0.001$; Figure 4). The inverse of the best fit slope (black line), $(8 \pm 1\text{ year})^{-1}$, should indicate the residence time of water in the ODZ, assuming that the measured nitrogen consumption rates give rise to the nitrogen deficit. This residence time is consistent with independent chlorofluorocarbon measurements (specific tracer for residence time) from the region, which suggest a residence time of 5–30 years [*Deutsch et al.*, 2001]. Moreover, there is additional structure observable, given the frequency of measurement with respect to depth. Adjacent samples, spaced ~4 m apart, show a different slope (Figure 4, grey contours) not significantly different from our modeled 296 day turnover time suggested for the nitrite turnover in the core of the ODZ (see section 4).

3.3. Nitrate Reduction and Nitrite Reoxidation Rate Measurements

Measurements of nitrate reduction to nitrite and nitrite reoxidation to nitrate were conducted at five selected depths corresponding to the top and bottom of the ODZ and at three intermediate depths within the ODZ (Figures 2c and 2d). The highest rates of both processes occurred at the top of the ODZ. The nitrate reduction rate decreased monotonically, from 120 ± 20 nmol L^{-1} d^{-1} at the top of the ODZ to 11 ± 3 nmol L^{-1} d^{-1} at the bottom. This profile appears to approximate a "Martin"-style power law dependence on organic matter supply [*Martin et al.*, 1987] as was observed for fixed nitrogen loss rates in the analogous ETNP [*Babbin et al.*, 2014]. Moreover, organic carbon-dependence has been discussed previously in the ETSP as being both the

limiting factor for nitrogen loss [*Ward et al.*, 2008] and the control of the entirety of anaerobic biogeochemistry [*Kalvelage et al.*, 2013]. Since nitrate concentration is not drawn down below 10 μmol L^{-1} within the ODZ, another factor such as organic carbon rain must limit the production of nitrite here.

Fitting a power law function through the nitrate reduction data (Figure 2c), the resulting best fit equation for reduction rate R as a function of depth z, with R_{top} and z_{top} corresponding to the upper ODZ boundary, is

$$R(z) = R_{top}\left(\frac{z}{z_{top}}\right)^{-1.23} \quad (p < 0.01)\ .$$

The power coefficient, −1.23 is similar to that derived in the ETNP for denitrification rates as dependent on organic matter fluxes (−1.3) [*Babbin et al.*, 2014] and reduced as expected compared to observations of organic matter remineralization in oxic waters [*Martin et al.*, 1987; *Van Mooy et al.*, 2002; *Hartnett and Devol*, 2003].

Nitrite reoxidation to nitrate also occurred at significant levels within the ODZ but was apparently most important at the upper and lower boundaries, where rates were 27 ± 6 nmol L^{-1} d^{-1} and 18 ± 5 nmol L^{-1} d^{-1}, respectively. Within the core of the ODZ, however, nitrite oxidation was minimal, 6 ± 1 nmol L^{-1} d^{-1} at the maximum nitrite concentration, and undetectable at the two other depths sampled. This observation from direct rate measurements corroborates many of the ideas put forward by *Casciotti et al.* [2013], who calculated that nitrite oxidation should be the major sink term of nitrite in the lower ODZ off of Peru and that nitrate reduction was larger than nitrite oxidation at the top of the ODZ. The absence of significant nitrite oxidation in the core of the ODZ is also corroborated by natural abundance isotope data collected simultaneously [*Peters et al.*, 2016]. Given the measured rates of anammox (<10 nmol N_2 L^{-1} d^{-1}) and the stoichiometry of nitrite oxidation by anammox (NO_2^- oxidation = 0.3 × N_2 production) [*Strous et al.*, 1998], anammox can be responsible for only a small fraction of the observed nitrite oxidation rates. These nitrite oxidation rates relative to nitrate reduction and nitrate resupply by physical processes maintain the nitrate concentrations observed in the ODZs.

3.4. Iodate as a Potential Oxidant for Nitrite

The addition of iodate increased the rates of nitrite oxidation, at least in samples from depths at which nitrite oxidation was detected in the control experiments (i.e., no amendments) (Figure 2d). In these experiments, iodate increased nitrite oxidation rates by 30 ± 20 nmol L^{-1} d^{-1} for the two shallowest depths. At the base of the ODZ, however, the rate increased with the addition of iodate by only 7 ± 7 nmol L^{-1} d^{-1}. There, the low in situ nitrite standing stock (0.3 μmol L^{-1}) and low nitrate reduction rates generating autochthonous nitrite are conceivably the limiting factors of reoxidation. Interestingly, at 250 and 350 m where no nitrite oxidation was detected in the control experiments, the addition of iodate did not stimulate any nitrite oxidation, suggesting that either the bacteria responsible for this coupling are not abundant within the core of the ODZ or that iodate alone did not induce a change in activity within the time frame of the experiments.

These results show that iodate-driven nitrite oxidation may be significant in the ODZ nitrite budget. In the ODZ of the Arabian Sea, iodide concentrations were observed to increase by up to 500 nmol L^{-1} between the oxygenated surface and anoxic core and comprise the entirety of the dissolved iodine pool within the ODZ [*Farrenkopf and Luther*, 2002]. A simple redox balance for the oxidation of nitrite by iodate results in a possible pathway of

$$3\ NO_2^- + IO_3^- \rightarrow 3NO_3^- + I^-\ .$$

This reaction is energetically favorable and yields ~50 kJ mol^{-1} of nitrite oxidized [*Garrels and Christ*, 1965; *Lam and Kuypers*, 2011]. As each iodate molecule can oxidize three nitrite molecules, the 500 nmol L^{-1} iodide accumulation can correspond to 1.5 μmol L^{-1} of nitrite consumption. Thus, the maximum nitrite concentration measured [*Farrenkopf and Luther*, 2002] in the Arabian Sea of 4.5 μmol L^{-1} might have been 33% larger without this process. As similar 500 nmol L^{-1} iodate concentrations occur in the oxygenated Pacific [*Nozaki*, 1997], the same potential seems likely to exist for the ETSP ODZ.

We note that another possible source of apparent anaerobic NO_2^- oxidation results from the reversibility of the nitrite oxidoreductase enzyme by which aerobic nitrifiers living at the ODZ boundary are ephemerally stressed by the lack of O_2 [*Kemeny et al.*, 2016]. However, given the consistency of the O_2 and NO_2^-

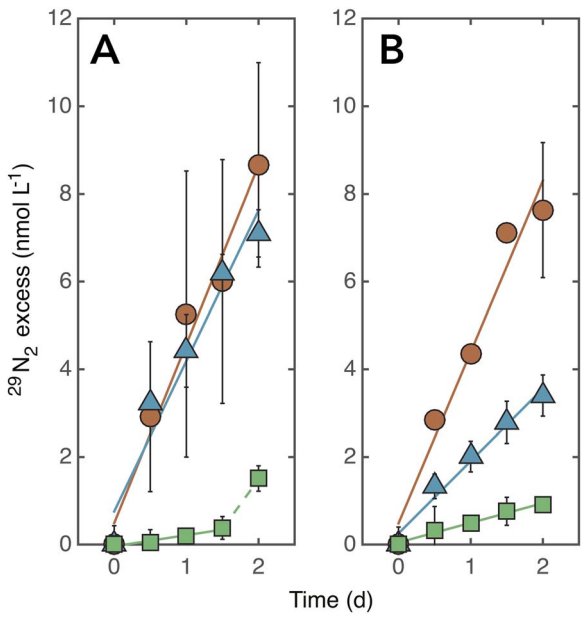

Figure 5. Rates of N_2 production from urea and its decay products. (a) Bottom of the oxycline, (b) depth of the SNM. Rates from ammonium (circles), cyanate (triangles), and urea (squares) are shown. The error bars denote standard deviations among triplicate time points, and the points without visible bars indicate that the error is smaller than the symbol.

concentration profiles, this explanation suggested by natural abundance isotope data for light-stressed nitrifiers in the high-O_2 Southern Ocean surface requires more investigation within ODZs. The stimulation by iodate here shows that iodate can play a role regardless of other complementary pathways by which NO_2^- may be oxidized in the absence of O_2.

3.5. Urea and Cyanate as Reduced Nitrogen Sources

It has been suggested that migrating zooplankton can increase anammox rates independently from denitrification by directly supplying an allochthonous source of ammonium independent from organic carbon [*Bianchi et al.*, 2014]. Urea, another significant excretion product of zooplankton and of larger migrating animals, may also augment nitrogen loss rates via anammox either through direct utilization or by the conversion of urea to ammonium and cyanate by other microbial clades or abiotically [*Kamennaya et al.*, 2008]. The productive upwelling zones of the eastern tropical Pacific, and particularly, the coastal ETSP studied here, are home to many cetaceans (both whales and dolphins). These mammals, which migrate frequently to depths between 80 and 150 m when foraging [*Williams et al.*, 2000; *Croll et al.*, 2001], in addition to zooplankton whose effect has been previously examined, may act as a direct injection source of urea to the top of the ODZ. Further, cyanate can form in seawater by many mechanisms related to primary productivity and organic matter degradation, including the decay of urea [*Kamennaya et al.*, 2008]. When urea decomposes, it is cleaved into one molecule each of ammonium and cyanate. We directly measured the response of N_2 production (presumably anammox; see below) rates to urea and cyanate at the base of the oxycline and at the depth of the SNM by using ^{15}N-labeled species of each of these substrates (Figure 5).

We found that cyanate could support significant anammox rates, especially at the base of the oxycline, where rates of cyanate oxidation to N_2 (3.4 ± 0.3 nmol L^{-1} d^{-1}) were comparable to those detected directly by labeled ammonium (4.1 ± 0.8 nmol L^{-1} d^{-1}). At the SNM, cyanate was still able to support anammox, albeit at reduced rates (1.5 ± 0.1 nmol L^{-1} d^{-1}) compared with ammonium (3.9 ± 0.3 nmol L^{-1} d^{-1}). Urea supported low N_2 production rates of 0.3 ± 0.1 and 0.4 ± 0.1 nmol L^{-1} d^{-1} for the oxycline and SNM samples, respectively. However, at the depth of the oxycline, an incubation artifact was observed, whereby urea supported N_2 production of 2.3 ± 0.5 nmol L^{-1} d^{-1} after a lag of 1.5 days. This stimulation, but only after 36 h, is indicative of a commonly observed bottle effect captured in incubations that isolate microbes from their full environment [*Holtappels et al.*, 2011].

We interpret these results as suggesting that cyanate can indeed be used as a source of reduced nitrogen for anammox, especially at the shallower depth where cyanate and urea productions are likely rapid due to sinking organic matter degradation [*Cho and Azam*, 1995; *Widner et al.*, 2016] and injections of urea from animals are more frequent. Although cyanate supported anammox rates immediately, anammox bacteria may not be directly responsible for this conversion because the full in situ microbial community is captured in the incubations. These results also show that urea cannot be used directly, but that presumably upon breakdown to ammonium and cyanate by urease produced by other organisms or some other biological or abiotic process, the substrate can be harnessed for N_2 generation. While the concentrations provided in the incubations are

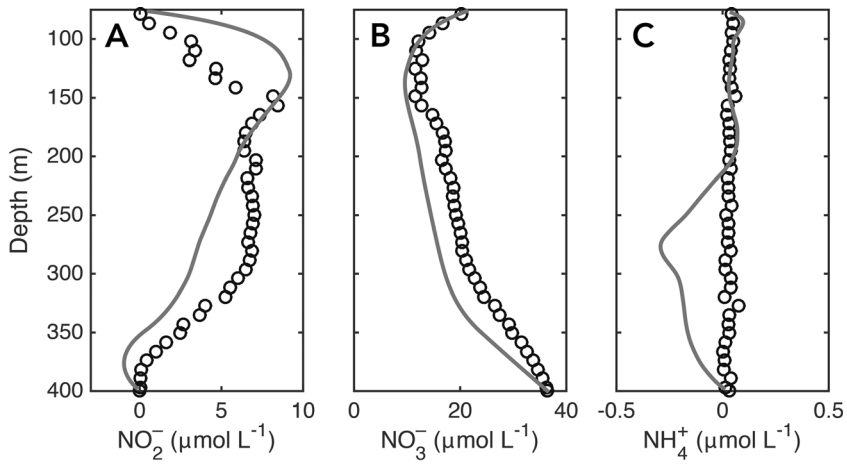

Figure 6. Modeled biogeochemical parameters within the anoxic layer (75–400 m). (a) Nitrite, (b) nitrate, and (c) ammonium. The circles denote measured concentrations during the pump cast, while the grey curves are the modeled distributions after 296 days of model integration.

greater than background and the measured rates were likely saturated, the in situ microorganisms appear to be primed to harness cyanate but not urea for N_2 production. Our results are supported by the transcriptome of the marine anammox bacterium *Candidatus Scalindua profunda* in which a putative cyanate hydratase was found to be highly expressed [*van de Vossenberg et al.*, 2013] but in which urease was not found. *Scalindua* is the only genus of anammox bacteria detected in ODZs on the basis of 16S rRNA identity [*Woebken et al.*, 2008; *Jayakumar et al.*, 2009]. As the cyanate hydratase enzyme converts cyanate to ammonium, it seems plausible that anammox bacteria containing this gene could access this pool as an indirect source of ammonium. Basic Local Alignment Search Tool (BLAST) searches [*Altschul et al.*, 1990, 1997] of metagenomic and metatranscriptomic data from the ETSP [*Stewart et al.*, 2011] also revealed sequences with similarity to putative cyanate hydratases (as determined by identity to Pfam entry PF02560; E value $< 10^{-5}$) from the *Scalindua* genome [*van de Vossenberg et al.*, 2013] and from *Nitrospina*, a genus of nitrite-oxidizing bacteria widely found in anoxic marine settings [*Fuchsman et al.*, 2011; *Füssel et al.*, 2011] that is genetically similar [*Lücker et al.*, 2013] to another nitrite oxidizer that has been recently shown to convert cyanate to ammonium [*Palatinszky et al.*, 2015]. We found potential cyanate hydratase sequences in the *Stewart et al.* [2011] ETSP metagenomes from all sampled depths above and within the ODZ (but not below). However, active expression indicated by hits to the metatranscriptome was only detected from the anoxic depths. Metatranscriptome hits also matched sequences from both *Scalindua* and *Nitrospina*. A complete table of BLAST hits is included in Table S1 in the supporting information.

4. Modeling of the Secondary Nitrite Maximum

From the observed depth dependencies of the five nitrite-affecting processes measured, parameterizations were developed to describe these rates in a one-dimensional model (Figure 2, grey lines). We used the observed power scaling best fit to our data to define the decrease of nitrate reduction rates with depth, set DNRA to zero throughout the water column, and linearly interpolated the measured nitrogen loss rates (Figure 2a) and partitioning (Figure 3) to 1 m resolution. We acknowledge that the partitioning between anammox and denitrification affects the model, but this distribution gives only slightly different results compared with allowing approximately equal rates of N_2 production by anammox and denitrification. Due to the unknown mechanism by which nitrite was oxidized to nitrate, however, we modeled its contribution to the nitrite budget conservatively with a stepwise function, dependent only upon the observed nitrite oxidation rate distribution.

Combining the effects of these biological rates together with vertical diffusion and advection, the model shows the chemical evolution of a parcel of water starting with no nitrite and a uniform nitrate deficit. The imbalance between the measured production of nitrite from nitrate reduction and its consumption via reoxidation and reduction by denitrification and anammox gives rise to a large secondary nitrite maximum (Figure 6a). The magnitude of the SNM keeps increasing with time, however, due to the

fact that the rates of the processes are not perfectly balanced at every depth. If these measured biological rates are assumed to be representative averages over time within the ODZ, then horizontal transport (which is ignored in the model) may be crucial to constraining the nitrite maximum. Nonetheless, the relative sizes of the modeled nitrate deficit (Figure 6b; up to 20 μmol L^{-1}) and corresponding nitrite accumulation (peak of 8.5 μmol L^{-1}) after 296 days of integration compare well to the observations, suggesting that these measured biological rates are reasonable in magnitude. The 296 days it takes to reproduce the nitrite maximum may in fact approximate the residence time of the water at this coastal site and is similar to that determined by *DeVries et al.* [2012] for the ETSP suboxic waters of 330 ± 150 days. ODZ residence time is, however, one of the most poorly constrained oceanographic parameters and is certainly dependent on the exact location within the ODZ.

Offsets between the modeled and measured nitrate and nitrite concentrations can be explained through differential lateral ventilation supplying different depth layers at slightly different rates (SI) and are supported by the physical structure of the water column (Figure S3). Of greater biogeochemical interest, however, is that the five rates as measured cause ammonium to be overconsumed in the lower ODZ and therefore require additional ammonium supply within the anoxic water column (Figure 6c).

Assuming a variable anammox contribution to nitrogen loss averaging ~50%, as evidenced by natural abundance nitrogen isotope data collected simultaneously [*Peters et al.*, 2016] and other tracer incubations at the same station (Figure 3), the 1-D model better reproduces the observed ammonium profile than if nitrogen loss is attributed to anammox alone (Figure S2), reducing the net average deficit across the ODZ by a factor of 10, from 0.85 μmol L^{-1} to 0.09 μmol L^{-1}. Still, not enough ammonium is generated in the lower ODZ. This is actually consistent with the possible role of additional reduced nitrogen sources to the lower ODZ, either through the direct excretion of ammonium [*Bianchi et al.*, 2014] or by the conversion of urea to ammonium and cyanate.

5. Anaerobic Nitrogen Cycle of the ETSP

The rate measurements presented here give a number of insights into the biogeochemical parameters controlling their distributions. These measurements provide reasonable first-order constraints on the development of the secondary nitrite maximum in the ETSP. Most of the inorganic nitrogen is rapidly recycled between nitrate and nitrite by coincident nitrate reduction and nitrite oxidation rates in the ODZ boundaries, and only a small portion of the nitrite is reduced by anammox and denitrification. Linking the high-resolution rate profile to passive chemical tracers leads to the following scenario of nitrite cycling in the ETSP:

1. Organic matter remineralization by nitrate reduction to nitrite with a standard power law distribution supplies nitrite for the other (nitrite-consuming) microbial processes.
2. Rates of nitrite reduction, namely, through anammox and denitrification, occur in ratios dictated by ammonium released by ammonification, with an additional source potentially required, either through low levels of autochthonous DNRA [*Lam et al.*, 2009] or a possible allochthonous source from migrating animals [*Bianchi et al.*, 2014] or advection offshore [*Kalvelage et al.*, 2013].
3. Anaerobic nitrite oxidation occurs at significant rates near the ODZ boundaries, where iodate can be a potential oxidant. However, iodate concentrations are likely to support a fraction of the entire process. Two other noteworthy oxidants that have been explored in ODZs, iron and manganese, are also insufficient to support the observed rates [*Glass et al.*, 2015; *Kondo and Moffett*, 2015]. Nitrite oxidoreductase reversibility may also play a role [*Kemeny et al.*, 2016].
4. Cycling between nitrate reduction and nitrite reoxidation at the boundaries supplies ammonium to support greater rates of anammox relative to denitrification. The increased contribution of anammox at the boundaries may potentially arise due to very low O_2 concentrations having a differential inhibitory effect on the two N_2 production pathways [*Dalsgaard et al.*, 2014].
5. The ETSP nitrite maximum is produced and actively maintained by an imbalance among the microbial rates of nitrate reduction, anammox, anaerobic nitrite oxidation, and physics; however, the ultimate reason for this imbalance, either a kinetic or thermodynamic control to maximize energy yield, remains to be elucidated.

Acknowledgments
We thank the captain and crew of the RVIB *Nathaniel B. Palmer* for assistance in sampling. We are grateful to Chief Scientist A.H. Devol for his advice and help onboard and to O. Ulloa and G. Alarcón for granting us access to the PPS and assistance in plumbing the system. We thank X. Peng for measuring the nitrate reduction samples and Q. Ji for measuring the nitrite oxidation samples. We are indebted to D. McRose for the metagenome searches and to B.X. Chang for her insight of iodate as a potential oxidant. This work was funded by NSF grants to B.B.W. (OCE-1029951), A.R.B (BIO-1402109), and C.W.M. (OCE-1233425). This publication was partially funded by the Joint Institute for the Study of the Atmosphere and Ocean (JISAO) under NOAA Cooperative Agreement NA10OAR4320148 and PMEL contribution number 4365 and JISAO contribution number 2447. Hydrographic and nutrient data are freely available at the NOAA NODC archive (NCEI Accession 0128141). All additional data may be obtained from A.R.B. (babbin@mit.edu).

References

Altschul, S. F., W. Gish, W. Miller, E. W. Myers, and D. J. Lipman (1990), Basic local alignment search tool, *J. Mol. Biol.*, *215*(3), 403–410.

Altschul, S. F., T. L. Madden, A. A. Schäffer, J. Zhang, Z. Zhang, W. Miller, and D. J. Lipman (1997), Gapped BLAST and PSI-BLAST: A new generation of protein database search programs, *Nucleic Acids Res.*, *25*(17), 3389–3402.

Amachi, S., N. Kawaguchi, Y. Muramatsu, S. Tsuchiya, Y. Watanabe, H. Shinoyama, and T. Fujii (2007), Dissimilatory iodate reduction by marine *Pseudomonas* sp. strain SCT, *Appl. Environ. Microbiol.*, *73*(18), 5725–5730, doi:10.1128/AEM.00241-07.

Babbin, A. R., R. G. Keil, A. H. Devol, and B. B. Ward (2014), Organic matter stoichiometry, flux, and oxygen control nitrogen loss in the ocean, *Science*, *344*(6182), 406–408.

Babbin, A. R., D. Bianchi, A. Jayakumar, and B. B. Ward (2015), Rapid nitrous oxide cycling in the suboxic ocean, *Science*, *348*(6239), 1127–1129, doi:10.1126/science.aaa8380.

Beman, J. M., J. Leilei Shih, and B. N. Popp (2013), Nitrite oxidation in the upper water column and oxygen minimum zone of the eastern tropical North Pacific Ocean, *ISME J.*, *7*(11), 2192–205, doi:10.1038/ismej.2013.96.

Bianchi, D., E. D. Galbraith, D. A. Carozza, K. A. S. Mislan, and C. A. Stock (2013), Intensification of open-ocean oxygen depletion by vertically migrating animals, *Nat. Geosci.*, *6*(7), 545–548, doi:10.1038/ngeo1837.

Bianchi, D., A. R. Babbin, and E. D. Galbraith (2014), Enhancement of anammox by the excretion of diel vertical migrators, *Proc. Natl. Acad. Sci. U.S.A.*, *111*(44), 15,653–15,658.

Bock, E., P. A. Wilderer, and A. Freitag (1988), Growth of *Nitrobacter* in the absence of dissolved oxygen, *Water Res.*, *22*(2), 245–250.

Brandes, J. A., and A. H. Devol (2002), A global marine-fixed nitrogen isotopic budget: Implications for Holocene nitrogen cycling, *Global Biogeochem. Cycles*, *16*(4), 67-1–67-14, doi:10.1029/2001GB001856.

Bristow, L. A., et al. (2016), Ammonium and nitrite oxidation at nanomolar oxygen concentrations in oxygen minimum zone waters, *Proc. Natl. Acad. Sci. U.S.A.*, *113*(38), 10,601–6, doi:10.1073/pnas.1600359113.

Buchwald, C., and K. L. Casciotti (2013), Isotopic ratios of nitrite as tracers of the sources and age of oceanic nitrite, *Nat. Geosci.*, *6*(4), 308–313, doi:10.1038/ngeo1745.

Buchwald, C., A. E. Santoro, R. H. R. Stanley, and K. L. Casciotti (2015), Nitrogen cycling in the secondary nitrite maximum of the Eastern Tropical North Pacific off Costa Rica, *Global Biogeochem. Cycles*, *29*, 2061–2081, doi:10.1002/2015GB005187.

Canfield, D. E., F. J. Stewart, B. Thamdrup, L. De Brabandere, T. Dalsgaard, E. F. Delong, N. P. Revsbech, and O. Ulloa (2010), A cryptic sulfur cycle in oxygen-minimum-zone waters off the Chilean Coast, *Science*, *330*(6009), 1375–1378, doi:10.1126/science.1196889.

Casciotti, K. L., C. Buchwald, and M. McIlvin (2013), Implications of nitrate and nitrite isotopic measurements for the mechanisms of nitrogen cycling in the Peru oxygen deficient zone, *Deep. Res. I*, *80*(C), 78–93, doi:10.1016/j.dsr.2013.05.017.

Chang, B. X., A. H. Devol, and S. R. Emerson (2010), Denitrification and the nitrogen gas excess in the Eastern Tropical South Pacific oxygen deficient zone, *Deep. Res. I*, *57*(9), 1092–1101, doi:10.1016/j.dsr.2010.05.009.

Cheung, W. W. L., V. W. Y. Lam, J. L. Sarmiento, K. Kearney, R. E. G. Watson, D. Zeller, and D. Pauly (2010), Large-scale redistribution of maximum fisheries catch potential in the global ocean under climate change, *Global Change Biol.*, *16*(1), 24–35, doi:10.1111/j.1365-2486.2009.01995.x.

Cho, B. C., and F. Azam (1995), Urea decomposition by bacteria in the Southern California Bight and its implications for the mesopelagic nitrogen cycle, *Mar. Ecol. Prog. Ser.*, *122*, 21–26.

Codispoti, L. A. (2007), An oceanic fixed nitrogen sink exceeding 400 Tg N a^{-1} vs the concept of homeostasis in the fixed-nitrogen inventory, *Biogeosciences*, *4*(2), 233–253.

Codispoti, L. A., J. A. Brandes, J. P. Christensen, A. H. Devol, S. W. A. Naqvi, H. W. Paerl, and T. Yoshinari (2001), The oceanic fixed nitrogen and nitrous oxide budgets: Moving targets as we enter the Anthropocene?, *Sci. Mar.*, *65*(S2), 85–105.

Croll, D. A., A. Acevedo-Gutiérrez, B. R. Tershy, and J. Urbán-Ramírez (2001), The diving behavior of blue and fin whales: Is dive duration shorter than expected based on oxygen stores?, *Comp. Biochem. Physiol. Part A Mol. Integr. Physiol.*, *129*(4), 797–809.

Dalsgaard, T., B. Thamdrup, L. Farías, and N. P. Revsbech (2012), Anammox and denitrification in the oxygen minimum zone of the eastern South Pacific, *Limnol. Oceanogr.*, *57*(5), 1331–1346, doi:10.4319/lo.2012.57.5.1331.

Dalsgaard, T., F. J. Stewart, B. Thamdrup, L. De Brabandere, N. P. Revsbech, O. Ulloa, D. E. Canfield, and E. F. DeLong (2014), Oxygen at nanomolar levels reversibly suppresses process rates and gene expression in anammox and denitrification in the oxygen minimum zone off northern Chile, *MBio*, *5*(6), e01966, doi:10.1128/mBio.01966-14.

De Brabandere, L., D. E. Canfield, T. Dalsgaard, G. E. Friederich, N. P. Revsbech, O. Ulloa, and B. Thamdrup (2014), Vertical partitioning of nitrogen-loss processes across the oxic-anoxic interface of an oceanic oxygen minimum zone, *Environ. Microbiol.*, *16*, 3041–3054, doi:10.1111/1462-2920.12255.

Deutsch, C., N. Gruber, R. M. Key, J. L. Sarmiento, and A. Ganachaud (2001), Denitrification and N2 fixation in the Pacific Ocean, *Global Biogeochem. Cycles*, *15*(2), 483–506, doi:10.1029/2000GB001291.

DeVries, T., C. Deutsch, F. Primeau, B. Chang, and A. Devol (2012), Global rates of water-column denitrification derived from nitrogen gas measurements, *Nat. Geosci.*, *5*(8), 547–550, doi:10.1038/ngeo1515.

Farrenkopf, A. M., and G. W. Luther (2002), Iodine chemistry reflects productivity and denitrification in the Arabian Sea: Evidence for flux of dissolved species from sediments of western India into the OMZ, *Deep Sea Res., Part II*, *49*(12), 2303–2318, doi:10.1016/S0967-0645(02)00038-3.

Farrenkopf, A. M., M. E. Dollhopf, S. N. Chadhain, G. W. Luther, and K. H. Nealson (1997), Reduction of iodate in seawater during Arabian Sea shipboard incubations and in laboratory cultures of the marine bacterium *Shewanella putrefaciens* strain MR-4, *Mar. Chem.*, *57*(3), 347–354.

Fennel, K., and E. Boss (2003), Subsurface maxima of phytoplankton and chlorophyll: Steady-state solutions from a simple model, *Limnol. Oceanogr.*, *48*(4), 1521–1534.

Friederich, G. E., and L. A. Codispoti (1987), An analysis of continuous vertical nutrient profiles taken during a cold-anomaly off Peru, *Deep Sea Res., Part A*, *34*(5), 1049–1065, doi:10.1016/0198-0149(87)90052-5.

Fuchsman, C. A., J. B. Kirkpatrick, W. J. Brazelton, J. W. Murray, and J. T. Staley (2011), Metabolic strategies of free-living and aggregate-associated bacterial communities inferred from biologic and chemical profiles in the Black Sea suboxic zone, *FEMS Microbiol. Ecol.*, *78*(3), 586–603, doi:10.1111/j.1574-6941.2011.01189.x.

Füssel, J., P. Lam, G. Lavik, M. M. Jensen, M. Holtappels, M. Günter, and M. M. M. Kuypers (2011), Nitrite oxidation in the Namibian oxygen minimum zone, *ISME J.*, *6*(6), 1200–1209, doi:10.1038/ismej.2011.178.

Garrels, R. M., and C. L. Christ (1965), *Solutions, Minerals, and Equilibria*, Freeman, Cooper & Company, San Francisco, Calif.

Glass, J. B., et al. (2015), Meta-omic signatures of microbial metal and nitrogen cycling in marine oxygen minimum zones, *Front. Microbiol.*, *6*, 998, doi:10.3389/fmicb.2015.00998.

Granger, J., and D. M. Sigman (2009), Removal of nitrite with sulfamic acid for nitrate N and O isotope analysis with the denitrifier method, *Rapid Commun. Mass Spectrom.*, *23*, 3753–3762, doi:10.1002/rcm.4307.

Grasshoff, K. (1983), Determination of nitrite, in *Methods of Seawater Analysis*, edited by K. Grasshoff, M. Ehrhardt, and K. Kremling, pp. 143–150, Verlag Chemie, Weinheim, Germany.

Griffin, B. M., J. Schott, and B. Schink (2007), Nitrite, an electron donor for anoxygenic photosynthesis, *Science*, *316*(5833), 1870, doi:10.1126/science.1139478.

Gruber, N. (2004), The dynamics of the marine nitrogen cycle and its influence on atmospheric CO2, in *The Ocean Carbon Cycle and Climate*, edited by M. Follows and T. Oguz, pp. 97–148, Kluwer Acad., Dordrecht, Netherlands.

Gruber, N., and J. L. Sarmiento (1997), Global patterns of marine nitrogen fixation and denitrification, *Global Biogeochem. Cycles*, *11*(2), 235–266, doi:10.1029/97GB00077.

Hamersley, M. R., et al. (2007), Anaerobic ammonium oxidation in the Peruvian oxygen minimum zone, *Limnol. Oceanogr.*, *52*(3), 923–933.

Hartnett, H. E., and A. H. Devol (2003), Role of a strong oxygen-deficient zone in the preservation and degradation of organic matter: A carbon budget for the continental margins of northwest Mexico and Washington State, *Geochim. Cosmochim. Acta*, *67*(2), 247–264, doi:10.1016/S0016-7037(02)01076-1.

Holtappels, M., G. Lavik, M. M. Jensen, M. M. M. Kuypers, and M. G. Klotz (2011), 15 N-labeling experiments to dissect the contributions of heterotrophic denitrification and anammox to nitrogen removal in the OMZ waters of the ocean, *Res. nitrification Relat. Process. Part A*, *223–251*, doi:10.1016/S0076-6879(11)86010-6.

Jayakumar, A., S. W. A. Naqvi, and B. B. Ward (2009), Distribution and relative quantification of key genes involved in fixed nitrogen loss from the Arabian Sea oxygen minimum zone, in *Indian Ocean Biogeochemcal Processes and Ecological Variability*, edited by J. D. Wiggert and R. R. Hood, pp. 187–203, AGU, Washington, D. C.

Ji, Q., A. R. Babbin, A. Jayakumar, S. Oleynik, and B. B. Ward (2015), Nitrous oxide production by nitrification and denitrification in the Eastern Tropical South Pacific oxygen minimum zone, *Geophys. Res. Lett.*, *42*, 10,755–10,764, doi:10.1002/2015GL066853.

Kalvelage, T., G. Lavik, P. Lam, S. Contreras, L. Arteaga, C. R. Löscher, A. Oschlies, A. Paulmier, L. Stramma, and M. M. M. Kuypers (2013), Nitrogen cycling driven by organic matter export in the South Pacific oxygen minimum zone, *Nat. Geosci.*, *6*, 228–234, doi:10.1038/ngeo1739.

Kamennaya, N. A., M. Chernihovsky, and A. F. Post (2008), The cyanate utilization capacity of marine unicellular cyanobacteria, *Limnol. Oceanogr.*, *53*(6), 2485–2494.

Kemeny, P. C., M. A. Weigand, R. Zhang, B. R. Carter, K. L. Karsh, S. E. Fawcett, and D. M. Sigman (2016), Enzyme-level interconversion of nitrate and nitrite in the fall mixed layer of the Antarctic Ocean, *Global Biogeochem. Cycles*, *30*, 1069–1085, doi:10.1002/2015GB005350.

Kondo, Y., and J. W. Moffett (2015), Iron redox cycling and subsurface offshore transport in the Eastern Tropical South Pacific oxygen minimum zone, *Mar. Chem.*, *168*, 95–103, doi:10.1016/j.marchem.2014.11.007.

Lam, P., and M. M. M. Kuypers (2011), Microbial nitrogen cycling processes in oxygen minimum zones, *Ann. Rev. Mar. Sci.*, *3*(1), 317–345, doi:10.1146/annurev-marine-120709-142814.

Lam, P., G. Lavik, M. M. Jensen, J. van de Vossenberg, M. Schmid, D. Woebken, D. Gutiérrez, R. Amann, M. S. M. Jetten, and M. M. M. Kuypers (2009), Revising the nitrogen cycle in the Peruvian oxygen minimum zone, *Proc. Natl. Acad. Sci.*, *106*(12), 4752–4757, doi:10.1073/pnas.0812444106.

Lam, P., M. M. Jensen, A. Kock, K. A. Lettmann, Y. Plancherel, G. Lavik, H. W. Bange, and M. M. M. Kuypers (2011), Origin and fate of the secondary nitrite maximum in the Arabian Sea, *Biogeosciences*, *8*(6), 1565–1577, doi:10.5194/bg-8-1565-2011.

Lees, H., and J. R. Simpson (1957), The biochemistry of the nitrifying organisms. V. Nitrite oxidation by *Nitrobacter*, *Biochem. J.*, *65*(2), 297–305.

Lipschultz, F., S. C. Wofsy, B. B. Ward, L. A. Codispoti, G. Friedrich, and J. W. Elkins (1990), Bacterial transformations of inorganic nitrogen in the oxygen-deficient waters of the Eastern Tropical South Pacific Ocean, *Deep. Res.*, *37*(10), 1513–1541.

Lomas, M. W., and F. Lipschultz (2006), Forming the primary nitrite maximum: Nitrifiers or phytoplankton?, *Limnol. Oceanogr.*, *51*(5), 2453–2467, doi:10.4319/lo.2006.51.5.2453.

Lücker, S., B. Nowka, T. Rattei, E. Spieck, and H. Daims (2013), The genome of *Nitrospina gracilis* illuminates the metabolism and evolution of the major marine nitrite oxidizer, *Front. Microbiol.*, *4*, 27, doi:10.3389/fmicb.2013.00027.

Martin, J. H., G. A. Knauer, D. M. Karl, and W. W. Broenkow (1987), VERTEX: Carbon cycling in the northeast Pacific, *Deep. Res.*, *34*(2), 267–285.

McIlvin, M. R., and M. A. Altabet (2005), Chemical conversion of nitrate and nitrite to nitrous oxide for nitrogen and oxygen isotopic analysis in freshwater and seawater, *Anal. Chem.*, *77*(17), 5589–5595, doi:10.1021/ac050528s.

Mordy, C. W., L. B. Eisner, P. Proctor, P. Stabeno, A. H. Devol, D. H. Shull, J. M. Napp, and T. Whitledge (2010), Temporary uncoupling of the marine nitrogen cycle: Accumulation of nitrite on the Bering Sea shelf, *Mar. Chem.*, *121*(1–4), 157–166, doi:10.1016/j.marchem.2010.04.004.

Newell, S. E., A. R. Babbin, A. Jayakumar, and B. B. Ward (2011), Ammonia oxidation rates and nitrification in the Arabian Sea, *Global Biogeochem. Cycles*, *25*, GB4016, doi:10.1029/2010GB003940.

Nozaki, Y. (1997), A fresh look at element distribution in the North Pacific Ocean, *Eos*, *Trans. Am. Geophys. Union*, *78*(21), 221–221, doi:10.1029/97EO00148.

Olson, R. J. (1981a), 15 N tracer studies of the primary nitrite maximum, *J. Mar. Res.*, *39*, 203–226.

Olson, R. J. (1981b), Differential photoinhibition of marine nitrifying bacteria: A possible mechanism for the formation of the primary nitrite maximum, *J. Mar. Res.*, *39*, 227–238.

Palatinszky, M., et al. (2015), Cyanate as an energy source for nitrifiers, *Nature*, *524*(7563), 105–108, doi:10.1038/nature14856.

Peng, X., C. A. Fuchsman, A. Jayakumar, S. Oleynik, W. Martens-Habbena, A. H. Devol, and B. B. Ward (2015), Ammonia and nitrite oxidation in the Eastern Tropical North Pacific, *Global Biogeochem. Cycles*, *29*, 2034–2049, doi:10.1002/2015GB005278.

Peng, X., C. A. Fuchsman, A. Jayakumar, M. J. Warner, A. H. Devol, and B. B. Ward (2016), Revisiting nitrification in the Eastern Tropical South Pacific: A focus on controls, *J. Geophys. Res. Oceans*, *121*, 1667–1684, doi:10.1002/2015JC011455.

Peters, B. D., A. R. Babbin, B. B. Ward, K. A. Lettman, C. W. Mordy, O. Ulloa, and K. L. Casciotti (2016), Vertical modeling of the nitrogen cycle in the Eastern Tropical South Pacific oxygen deficient zone using high resolution concentration and isotope measurements, *Global Biogeochem. Cycles*, *30*, 1661–1681, doi:10.1002/2016GB005415.

Revsbech, N. P., L. H. Larsen, J. Gundersen, T. Dalsgaard, O. Ulloa, and B. Thamdrup (2009), Determination of ultra-low oxygen concentrations in oxygen minimum zones by the STOX sensor, *Limnol. Oceanogr. Methods*, *7*, 371–381.

Sigman, D. M., K. L. Casciotti, M. Andreani, C. Barford, M. Galanter, and J. K. Böhlke (2001), A bacterial method for the nitrogen isotopic analysis of nitrate in seawater and freshwater, *Anal. Chem.*, *73*(17), 4145–4153, doi:10.1021/ac010088e.

Steinberg, D. K., S. A. Goldthwait, and D. A. Hansell (2002), Zooplankton vertical migration and the active transport of dissolved organic and inorganic nitrogen in the Sargasso Sea, *Deep Sea Res., Part I*, *49*(8), 1445–1461, doi:10.1016/S0967-0637(02)00037-7.

Stewart, F. J., O. Ulloa, and E. F. DeLong (2011), Microbial metatranscriptomics in a permanent marine oxygen minimum zone, *Environ. Microbiol.*, *14*(1), 23–40, doi:10.1111/j.1462-2920.2010.02400.x.

Strickland, J. D. H., and T. R. Parsons (1972), *A Practical Handbook of Seawater Analysis*, 2nd ed., Fisheries Research Board of Canada, Ottawa.

Strous, M., J. J. Heijnen, J. G. Kuenen, and M. S. M. Jetten (1998), The sequencing batch reactor as a powerful tool for the study of slowly growing anaerobic ammonium-oxidizing microorganisms, *Appl. Microbiol. Biotechnol.*, *50*(5), 589–596.

Thamdrup, B., T. Dalsgaard, M. M. Jensen, O. Ulloa, L. Farías, and R. Escribano (2006), Anaerobic ammonium oxidation in the oxygen-deficient waters off northern Chile, *Limnol. Oceanogr.*, *51*(5), 2145–2156.

Tiano, L., E. Garcia-Robledo, T. Dalsgaard, A. H. Devol, B. B. Ward, O. Ulloa, D. E. Canfield, and N. Peter Revsbech (2014), Oxygen distribution and aerobic respiration in the north and south eastern tropical Pacific oxygen minimum zones, *Deep Sea Res., Part I*, *94*, 173–183, doi:10.1016/j.dsr.2014.10.001.

van de Vossenberg, J., et al. (2013), The metagenome of the marine anammox bacterium "*Candidatus Scalindua profunda*" illustrates the-versatility of this globally important nitrogen cycle bacterium, *Environ. Microbiol.*, *15*(5), 1275–1289, doi:10.1111/j.1462-2920.2012.02774.x.

Van Mooy, B. A. S., R. G. Keil, and A. H. Devol (2002), Impact of suboxia on sinking particulate organic carbon: Enhanced carbon flux and preferential degradation of amino acids via denitrification, *Geochim. Cosmochim. Acta*, *66*(3), 457–465.

Ward, B. B. (2013), How nitrogen is lost, *Science*, *341*(6144), 352–3, doi:10.1126/science.1240314.

Ward, B. B., C. B. Tuit, A. Jayakumar, J. J. Rich, J. Moffett, and S. W. A. Naqvi (2008), Organic carbon, and not copper, controls denitrification in oxygen minimum zones of the ocean, *Deep Sea Res., Part I*, *55*(12), 1672–1683.

Ward, B. B., A. H. Devol, J. J. Rich, B. X. Chang, S. E. Bulow, H. Naik, A. Pratihary, and A. Jayakumar (2009), Denitrification as the dominant nitrogen loss process in the Arabian Sea, *Nature*, *461*(7260), 78–81, doi:10.1038/nature08276.

Widner, B., M. R. Mulholland, and K. Mopper (2016), Distribution, sources, and sinks of cyanate in the coastal North Atlantic Ocean, *Environ. Sci. Technol. Lett.*, doi:10.1021/acs.estlett.6b00165.

Williams, T. M., R. W. Davis, L. A. Fuiman, J. Francis, B. J. Le, M. Horning, J. Calambokidis, and D. A. Croll (2000), Sink or swim: Strategies for cost-efficient diving by marine mammals, *Science*, *288*(5463), 133–136, doi:10.1126/science.288.5463.133.

Wishner, K. F., M. M. Gowing, and C. Gelfman (1998), Mesozooplankton biomass in the upper 1000 m in the Arabian Sea: Overall seasonal and geographical patterns, and relationship to oxygen gradients, *Deep Sea Res., Part II*, *45*(10–11), 2405–2432, doi:10.1016/S0967-0645(98)00078-2.

Wishner, K. F., C. Gelfman, M. M. Gowing, D. M. Outram, M. Rapien, and R. L. Williams (2008), Vertical zonation and distributions of calanoid copepods through the lower oxycline of the Arabian Sea oxygen minimum zone, *Prog. Oceanogr.*, *78*(2), 163–191, doi:10.1016/j.pocean.2008.03.001.

Wishner, K. F., D. M. Outram, B. A. Seibel, K. L. Daly, and R. L. Williams (2013), Zooplankton in the eastern tropical North Pacific: Boundary effects of oxygen minimum zone expansion, *Deep Sea Res., Part I*, *79*, 122–140, doi:10.1016/j.dsr.2013.05.012.

Woebken, D., P. Lam, M. M. M. Kuypers, S. W. A. Naqvi, B. Kartal, M. Strous, M. S. M. Jetten, B. M. Fuchs, and R. Amann (2008), A microdiversity study of anammox bacteria reveals a novel *Candidatus Scalindua* phylotype in marine oxygen minimum zones, *Environ. Microbiol.*, *10*(11), 3106–3119, doi:10.1111/j.1462-2920.2008.01640.x.

Yamagishi, H., M. B. Westley, B. N. Popp, S. Toyoda, N. Yoshida, S. Watanabe, K. Koba, and Y. Yamanaka (2007), Role of nitrification and denitrification on the nitrous oxide cycle in the eastern tropical North Pacific and Gulf of California, *J. Geophys. Res.*, *112*, G02015, doi:10.1029/2006JG000227.